Spectral correlation of four wave mixing generated in a photonic crystal fiber pumped by a chirped pulse

PAUL ROBERT,[1] CORALIE FOURCADE-DUTIN,[1-2] ROMAIN DAULIAT,[3] RAPHAEL JAMIER,[3] HECTOR MUÑOZ-MARCO,[4] PERE PEREZ-MILLAN,[4] JOHN M. DUDLEY,[1] PHILIPPE ROY,[3] HERVE MAILLOTTE,[1] DAMIEN BIGOURD[1-2*]

[1]Institut FEMTO-ST, Département d'Optique, UMR CNRS 6174 -Université Bourgogne Franche-Comté, 25030 Besançon, France
[2]Laboratoire IMS, UMR CNRS 5218, University of Bordeaux, 33400 Talence, France
[3]Université Limoges, XLIM, UMR CNRS 7252, F-87000 Limoges, France
[4]FYLA LASER SL, Ronda Guglielmo Marconi 12, 46980, Paterna (Valencia), Spain
*Corresponding author: damien.bigourd@u-bordeaux.fr

The spectral correlation of four-wave mixing in a photonic crystal fiber pumped by a chirped pulse has been measured using the dispersive Fourier transform method. From statistical measurements of multiple shot-to-shot spectral measurements, the spectral correlation between the signal and idler photons reveals physical insights into the particular portion of the pump spectrum responsible for generating the FWM

Pulse amplification through four wave mixing (FWM) in optical fiber has been extensively investigated for important applications linked with its large gain-bandwidth [1], high gain [2] and very wide tunability [3]. When the pulses involved in the process have a high peak power, the pulses are initially stretched before being injected in the fiber [4, 5, 6] such that the FWM process can be achieved in a fiber with a silica core, even for a pulse energy in the microjoule level [7,8,9]. For a chirped pump pulse, the instantaneous frequencies are temporally dispersed and the spontaneous photons are generated with temporal and spectral distributions according to phase-matched FWM relation [10]. Significantly, we have shown that this configuration yields a very large gain bandwidth [2] that enables ultra-short pulse amplification [1]. However, the injected signal requires chirp optimization to match the temporal distribution of the parametric gain spectrum, which depends on both the pump and fiber properties [1]. Therefore, this parametric gain distribution needs to be understood and characterized to efficiently design a broadband amplifier.

Although some previous studies have used a pump-probe technique to study the gain distribution, this method is experimentally complex, which limits it broad use in studying

chirped-pulse FWM over wider parameter ranges [11]. In this work, we present a much simpler approach that allows the spectral and temporal distribution of the instantaneous parametric process to be studied using the dispersive Fourier transformation (DFT) method [12]. This powerful technique is significantly simpler to implement since it provides the desired information without the need to inject a suitable signal, and also readily allows statistical correlation data to be extracted.

The DFT method exploits time to frequency mapping to allow real time measurement of single-shot spectral fluctuations. DFT has been widely used to study a range of physical processes in fiber such as rogue wave dynamics, continuum generation and spontaneous FWM [13-18]. In our case, we use DFT to measure the spectral correlation between the FWM side bands generated from a chirped pump pulse, representing a new application of this method, and one which allows us to determine physical insights into the particular portion of the pump spectrum responsible for generating the FWM. In particular, for degenerate FWM, two pump photons are converted to signal and idler photons, with spontaneous generation achieved from different possibilities depending on phase matching criteria. This leads to an asymmetry in the FWM band in a single shot spectrum measurement [16]. Once the shots are averaged, the shape of the spontaneous FWM spectrum should represent the gain profile of the parametric amplification in the unsaturated regime. In the following, we exploit the DFT statistical measurements over many single shot spectra to correlate the signal and idler photons and to infer the origin of the FWM within the pump.

We firstly illustrate the principle of this method using numerical simulations based on integrating the nonlinear Schrödinger equation using the split step method. The parameters used were as follows. The input chirped pump pulse has duration of $\Delta t=50$ ps and spectral bandwidth $\Delta\lambda$ of 6 nm centered at 1030 nm. This corresponds to a chirp of $\Delta\tau/\Delta\lambda$=-8.3 ps/nm. The pulse is injected in a 5-meter-long photonic crystal fiber (PCF) which has a nonlinear

coefficient of 11 W^{-1}.km^{-1} and a zero-dispersion wavelength (ZDW) at 1028 nm. This means that only part of the pump spectrum lies in the anomalous dispersion regime. 500 simulations have been performed with random noise initial condition by adding half photon per temporal mode. Figure 1 shows a spectrogram of the average electric field at the fiber output for input peak power Pp=120 W. The red line corresponds to the pump pulse. As it is chirped, the instantaneous pump wavelengths are linearly spread in the temporal envelope. The temporal and spectral axis (top and bottom) are therefore linked by the chirp value; i.e $\Delta\tau/\Delta\lambda$. For each delay, the pump has a particular instantaneous wavelength and a pump power that creates a FWM with specific properties [2]. Indeed, two specific FWM bands are generated with different spectral locations and bandwidth. For example, at the pump wavelengths of 1030 nm (t=0 ps) and 1032 nm (-16.6 ps), the two lobes are located at ~1078/986 nm and 1061/998nm, respectively.
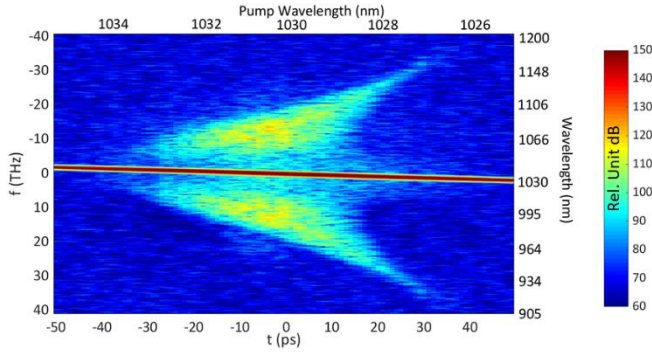

Fig. 1. Spectrogram of the averaged electric field at the PCF output for Pp=120 W.

To analyse the shot to shot fluctuations statistically, the spectral correlation $\rho(\lambda_1, \lambda_2)$ has been calculated between any two wavelengths λ_1 and λ_2 according to

$$\rho(\lambda_1, \lambda_2) = \frac{\langle I(\lambda_1)I(\lambda_2)\rangle - \langle I(\lambda_1)\rangle\langle I(\lambda_2)\rangle}{\sqrt{\langle I^2(\lambda_1)\rangle - \langle I(\lambda_1)\rangle^2 \cdot \langle I^2(\lambda_2)\rangle - \langle I(\lambda_2)\rangle^2}}$$ (1)

where the angle brackets represent an ensemble average. The correlation ρ varies from -1 to +1 indicating intensity fluctuations in the opposite or same directions respectively. For ρ=0, no correlation exists between λ_1 and λ_2. The spectral correlation between the lower and higher parts of the spectrum is shown in Fig. 2 together with the average spectra. The red line (top-right) corresponds to the positive correlation of the pump spectrum with itself; i.e the auto-correlation. Since the FWM process is originated from a depletion of the pump, the correlation between the side bands and the pump is negatively correlated (ρ~-0.3).

As the two axes represent the wavelength of the signal λ_s and idler λ_i, the theoretical relationship of FWM from energy conservation ($2/\lambda_p=1/\lambda_s+1/\lambda_i$) can be also plotted. The black curves in Fig. 2 represent three cases for a selection of pump wavelengths λ_p, and we can see from these results how it is possible to infer the particular pump component, which generates the FWM bands. For example, when the fiber is pumped by a chirped pulse with Pp=120 W (Fig. 2(a)), the bands at ~980 nm and 1000 nm are mostly generated from the pump part at 1030 nm lying in the anomalous dispersion regime. The photons in the range of 930-980 nm and 1090-1140 nm are generated from the pump between 1025-1030

nm. These observations are in very good agreement with those from the spectrogram (Fig. 1). We have also checked that the Raman effect does not affect this distribution.
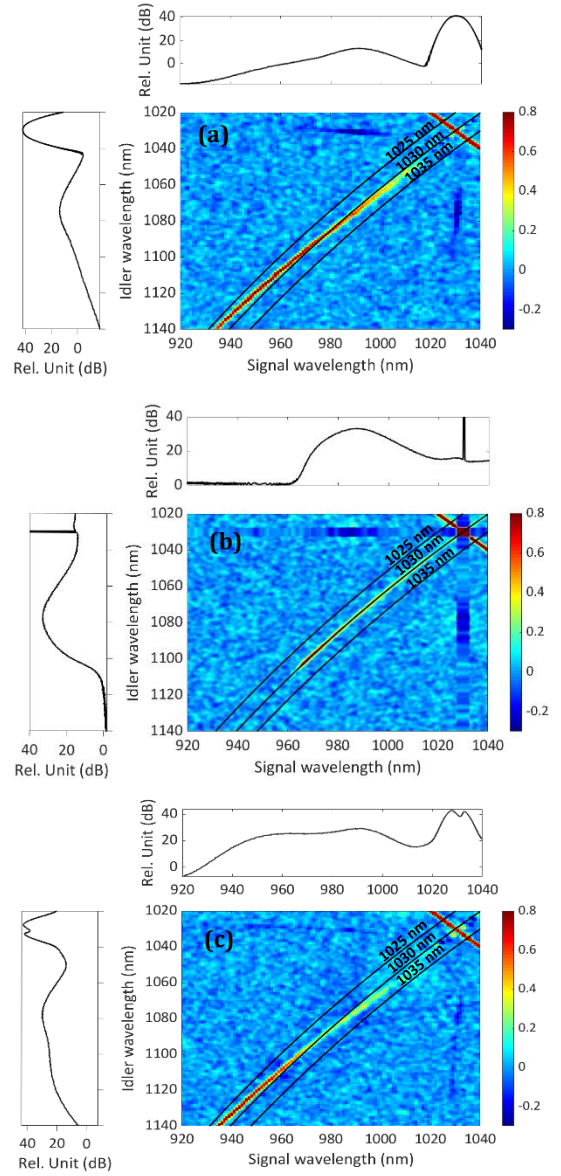

Fig. 2. Spectral correlation between the Stokes and Anti-Stokes for a) Pp=120W and a chirped pump pulse, b) for Pp=120W and a monochromatic pump c) for Pp=220W and a chirped pump pulse. The average spectra are displayed for all cases as top and left inserts. The black lines are plotted from the photon energy conservation law for several pump wavelengths.

To gain further insight, we performed the simulations under the same conditions but with a monochromatic pump (Fig. 2(b)). Compared to the previous case, the bandwidths are lower since the FWM photons are generated from the pump with a narrow spectrum. Indeed, the spectral correlation is along the black line plotted from the energy conservation law for λ_p=1030 nm. The numerical results for a chirped pulse with Pp=220 W (Fig. 2(c)) show that the FWM bands increase and the pump is affected by self

phase modulation (SPM). In this case, the ρ value decreases for the pump wavelength higher than 1030 nm and corresponds to the hole in the pump spectrum.

Our experimental setup is shown in Fig. 3a. The pump pulse is generated from a mode-locked oscillator (Flint, LightConversion) delivering a train of pulses at 76 MHz with a duration of 80 fs at FWHM centered at 1030 nm. The total average power is 1.5 W. A part of the oscillator output (around 750 mW) seeds the pump chain via a stretching stage composed of a volume Bragg grating (VBG) that stretches the pulses to a duration of ~50 ps (FWHM), an acoustooptic modulator (AOM) to decrease the repetition rate to 1 MHz and several ytterbium doped fiber amplifiers (YDFA) to progressively increase the average power up to 1 W. The pulse bandwidth (FWHM) at the output of the amplifier is ~ 9 nm and is modulated due to SPM. The pump pulse is then injected in a 5-meter-long PCF which has the same dispersion profile as the one used in the simulations. Two FWM lobes are generated in the PCF and are located at 1001 and 1071 nm for an average power of 18 mW (Fig. 3(b)).
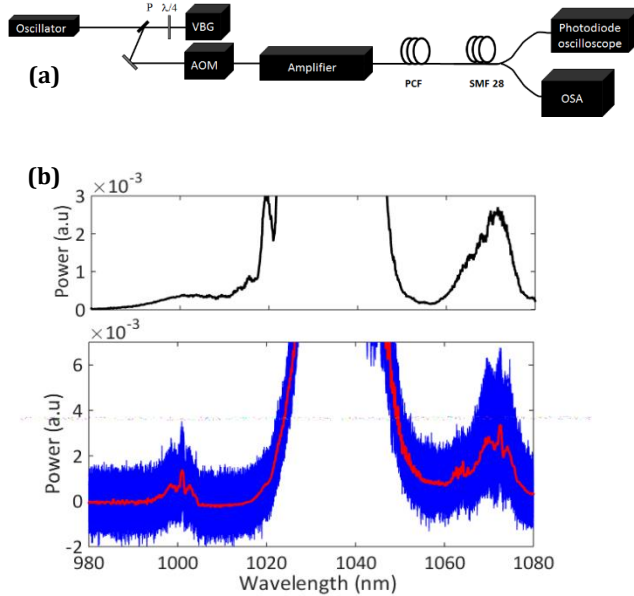

(a)

(b)

Fig. 3. Experimental set-up. VBG, Volume Bragg Grating; AOM, acousto-optic modulator; PCF Photonic Crystal Fiber; OSA, Optical Spectrum Analyzer et b)FWM bands detected with an OSA (black line) and with the DFT set-up. The averaged spectrum (red line) of 500 single shots (blue lines) are displayed.

In order to record single shot spectra, a dispersive Fourier transform set-up has been implemented at the PCF output. The beam is injected in an 11.5 km long fiber (SMF28) to stretch the output with approximate chirp value of ~-2.54 nm/ns. Thus, the delay between the two sidebands is ~27 ns. The output is detected with a fast photodiode and an oscilloscope with a maximum bandwidth of 12 GHz. For the following, we use a limited number of points to 5×10^6 for the 500 pulses corresponding to a spectral resolution of ~0.25 nm. Figure 3(b) displays the superposition of 500 single shot spectra (blue lines) and the averaged curve. To accurately reconstruct the DFT time-frequency mapping, we used both second and third order dispersion coefficients of the SMF (β_2=17 ps^2/km, β_3=-0.0134 ps^3/km) in the analysis of the

experimental data [12]. From Figure 3(b) (blue lines), we can see the large shot to shot fluctuation of the sideband but a good agreement is obtained between the average spectrum (red line) and the curve measured by an optical spectrum analyzer (black line). Figure 4 shows the spectral correlation map between 980 and 1090 nm for an average power of 24 mW. As expected, the pump spectrum is positively correlated with itself and the correlation between two identical FWM bands corresponds to a positive line with a maximum ρ value equal to 1. From Eq. 1, the correlation map is symmetric about the correlated positive diagonal. As the Stokes and anti-Stokes photons are degenerate from the depletion of the pump pulse, an anti-correlation between the pump and the two side lobes are observed (black dashed squares) [13]. In the following, we will focus on the correlation between the two FWM bands (black squares).
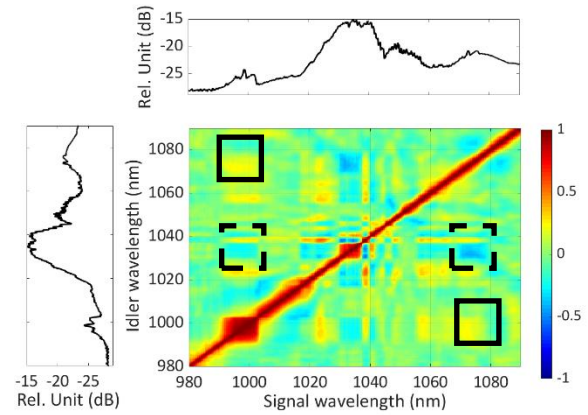

Fig. 4. Spectral correlation map of the full spectrum for a power of 24 mW. The black dashed squares correspond to the correlation between the pump and the FWM bands while the black squares show the correlation between the two bands.

The spectral correlations between the two side bands (black squares in Fig. 4) are also shown in Fig. 5 for an average power of 18 mW and 24 mW. The black lines are plotted from the photon energy conservation law for the pump wavelength of 1025, 1030 and 1035 nm. The correlation spectral maps have a different shape from the one predicted by the numerical simulations (Fig. 2), attributed to structure on the pump pulse used in the experiments or uncertainties in the fiber dispersion curve. From a pump-probe experiment [11], we have also observed similar behavior with another PCF. At a power of 18 mW, a positive value is observed with a specific shape. The maximum at ρ~0.4 corresponds to the correlation between the two parts 1068-1071nm/990-997nm. These parts of the bands are mainly generated from the pump spectrum around 1030 nm. Another positive ρ value (~0.25) located between 1073-1075/997-1002 is also obtained and these FWM bands are mostly generated from the pump spectrum at ~1035 nm. Surprisingly, the correlated bands are not symmetric around the pump spectrum; i.e the furthest part in one side is correlated to the closest part in the other side. This information cannot be obtained directly from a standard spectrometer.

At higher pump power, the side bands are shifted away from the pump and the positive correlation is mainly between 1070-1075 nm and 995-1005 nm. A negative correlation value (ρ=-0.15) at around 1082 nm is also observed. This is attributed to SPM accumulated by the pump that decreases the correlation value.

From the black line (Fig. 5(b)), we can deduce that it originates from the pump spectrum at >1035 nm. Indeed, a spectral hole in the pump is observed at 1037 nm (Fig. 4) and is consistent with the signature of the decrease in correlation as expected from the simulations.
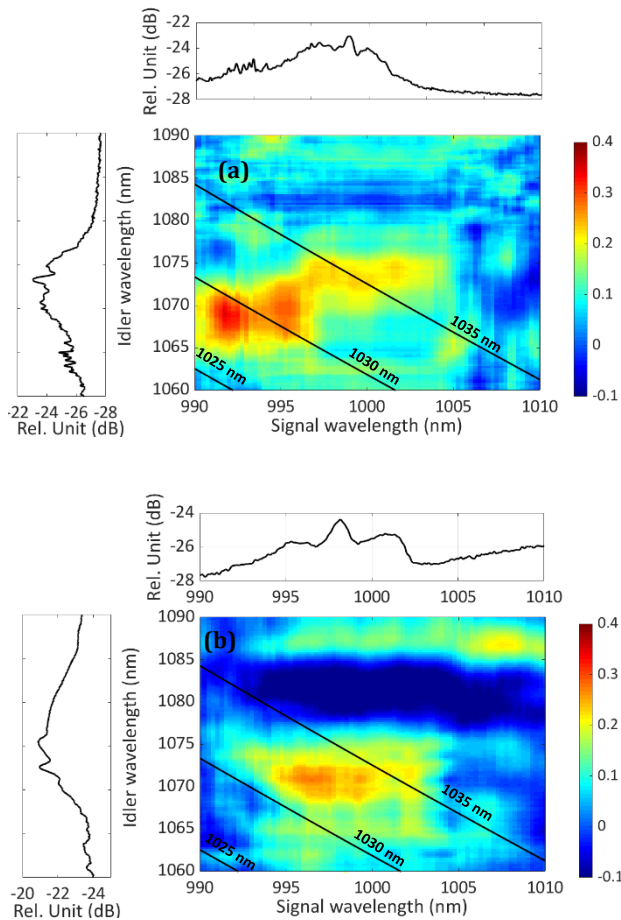

Fig. 5. Spectral correlation between the Stokes and Anti-Stokes for a power of 18 mW (a) and 24 mW (b). The average spectrum are displayed for each cases. The black lines are plotted from the photon energy conservation law for several pump wavelengths.

In conclusion, we have shown that the DFT method can be implemented to measure the spectral correlation between side bands. In the case of a chirped pump pulse, the spectral correlation map can be used to infer the pump part that generated the FWM. This method is relatively straightforward since it requires only one pump pulse without any seed injection. In addition, the statistical analysis provides significant new information and therefore the DFT method can be used as a highly complementary diagnostic to standard spectrometers. We believe that it will be of prime interest for the development of fiber amplifier supporting a very broad bandwidth [1].

REFERENCES

1. C Fourcade-Dutin, O Vanvincq, A Mussot, E Hugonnot and D Bigourd, J. Opt. Soc. Am B **32**, 1488 (2015).
2. O Vanvincq, C Fourcade-Dutin, A Mussot, E Hugonnot and D Bigourd, J. Opt. Soc. Am B **32**, 1479 (2015).
3. Y. Zhou, K. K. Y. Cheung, S. Yang, P. C. Chui and K. K. Y. Wong, Opt. Lett. **34**, 989 (2009).
4. D. Bigourd, L. Lago, A. Mussot, A. Kudlinski, J.F. Gleyze and E. Hugonnot, Opt. Lett. **35**, 3840 (2010).
5. Y. Qin, O. Batjargal, B. Cromey and K. Kieu, Opt. Exp. **28**, 2317 (2020).
6. Y. Qin, Y.H Ou, B. Cromey, O. Batjargal, J. K. Barton and K. Kieu, Opt. Lett. **44**, 3422 (2019).
7. W. Fu and F.W. Wise, Opt. Lett. **43**, 5331 (2018).
8. P. Morin, J. Dubertrand, P. Beaure d'Augeres, Y. Quiquempois, G. Bouwmans, A. Mussot and E. Hugonnot, Opt. Lett. **43**, 4683 (2018).
9. D. Bigourd, P. Morin, J. Dubertrand, C. Fourcade-Dutin, H. Maillotte, Y Quiquempois, G. Bouwmans and E. Hugonnot, IEEE Photon. Technol. Lett. **31**, 214 (2018).
10. D. Bigourd, P. Beaure d'Augeres, J. Dubertrand, E. Hugonnot and A. Mussot, Opt. Lett. **39**, 3782 (2014).
11. C. Fourcade-Dutin, A. Imperio, R. Dauliat, R. Jamier, H. Muñoz-Marco, P. Pérez-Millán, H. Maillotte, P. Roy and D. Bigourd, Photonics **6**, 20 (2019).
12. K. Goda and B. Jalali, Nat. Photonics **7**, 102 (2013).
13. P. Béjot, J. Kasparian, E. Salmon, R. Ackermann and J.-P Wolf, Appl. Phys. B **87**, 1 (2007).
14. B. Wetzel, A. Stefani, L. Larger, P. A. Lacourt, J. M. Merolla, T. Sylvestre, A. Kudlinski, A. Mussot, G. Genty, F. Dias and J. M. Dudley, Sc. Reports **2**, 882 (2012).
15. M. Narhi, B. Wetzel, C. Billet, S. Toenger, T. Sylvestre, J.M. Merolla, R. Morandotti, F. Dias, G. Genty and J. Dudley, Nat. Communications **7**, 13675 (2016).
16. D. R. Solli, G. Herink, B. Jalali and C. Ropers, Nat. Photonics **6**, 463 (2012).
17. X. Wang, D. Bigourd, A. Kudlinski,K. K. Y. Wong, M. Douay, L. Bigot, A. Lerouge, Y. Quiquempois, and A. Mussot, Opt. Lett. **39**, 1881 (2014).
18. T. Godin, B. Wetzel, T. Sylvestre, L. Larger, A. Kudlinski, A. Mussot, A. Ben Salem, M. Zghal, G. Genty, F. Dias, and J. M. Dudley, Opt. Exp. **21**, 18452 (2013).

REFERENCES

1. C Fourcade-Dutin, O Vanvincq, A Mussot, E Hugonnot, D Bigourd, "Ultrabroadband fiber optical parametric amplifiers pumped by chirped pulses. Part 2: sub-30 fs pulse amplification at high gain," J. Opt. Soc. Am B **32**, 1488 (2015).

2. O Vanvincq, C Fourcade-Dutin, A Mussot, E Hugonnot, D Bigourd, "Ultrabroadband fiber optical parametric amplifiers pumped by chirped pulses. Part 1: analytical model," J. Opt. Soc. Am B **32**, 1479 (2015).

3. Y. Zhou, K. K. Y. Cheung, S. Yang, P. C. Chui, K. K. Y. Wong, "Widely tunable picosecond optical parametric oscillator using highly nonlinear fiber," Opt. Lett. **34**, 989 (2009) .

4. D. Bigourd, L. Lago, A. Mussot, A. Kudlinski, J.F. Gleyze, E. Hugonnot, "High-gain fiber optical parametric chirped pulse amplification of femtosecond pulses at 1 μm," Opt. Lett. **35**, 3840 (2010).

5. Y. Qin, O. Batjargal, B. Cromey, K. Kieu, "All-fiber high-power 1700 nm femtosecond laser based on optical parametric chirped-pulse amplification," Opt. Exp. **28**, 2317 (2020)

6. Y. Qin, Y.H Ou, B. Cromey, O. Batjargal, J. K. Barton, K. Kieu, "Watt-level all-fiber optical parametric chirped-pulse amplifier working at 1300 nm," Opt. Lett. 44, 3422 (2019).

7. W. Fu, F.W. Wise, "Normal-dispersion fiber optical parametric chirped-pulse amplification," Opt. Lett. **43**, 5331 (2018).

8. P. Morin, J. Dubertrand, P. Beaure d'Augeres, Y. Quiquempois, G. Bouwmans, A. Mussot, E. Hugonnot, "μJ-level Raman-assisted fiber optical parametric chirped-pulse amplification**,**" Opt. Lett. **43**, 4683 (2018).

9. D. Bigourd, P. Morin, J. Dubertrand, C. Fourcade-Dutin, H. Maillotte, Y Quiquempois, G. Bouwmans, E. Hugonnot, "Parametric gain shaping from a structured pump pulse," IEEE Photon. Technol. Lett. **31**, 214 (2018).

10. D. Bigourd, P. Beaure d'Augeres, J. Dubertrand, E. Hugonnot, A. Mussot, "Ultra-broadband fiber optical parametric amplifier pumped by chirped pulses," Opt. Lett. **39**, 3782 (2014).

11. C. Fourcade-Dutin, A. Imperio, R. Dauliat, R. Jamier, H. Muñoz-Marco, P. Pérez-Millán, H. Maillotte, P. Roy, D. Bigourd, "Temporal Distribution Measurement of the Parametric Spectral Gain in a Photonic Crystal Fiber Pumped by a Chirped Pulse," Photonics **6**, 20 (2019).

12. K. Goda and B. Jalali, "Dispersive Fourier transform for fast continuous single-shot measurements," Nature Photonics **7**, 102 (2013).

13. P. Béjot, J. Kasparian, E. Salmon, R. Ackermann, J.-P Wolf, "Spectral correlation and noise reduction in laser filaments," Appl. Phys. B **87**, 1 (2007).

14. B. Wetzel, A. Stefani, L. Larger, P. A. Lacourt, J. M. Merolla, T. Sylvestre, A. Kudlinski, A. Mussot, G. Genty, F. Dias, J. M. Dudley, "Real-time full bandwidth measurement of spectral noise in supercontinuum generation," Scientific Reports **2**, 882 (2012).

15. M. Narhi, B. Wetzel; C. Billet, S. Toenger, T. Sylvestre, J.M. Merolla, R. Morandotti, F. Dias, G. Genty, J. Dudley, "Real-time measurements of spontaneous breathers and rogue wave events in optical fibre modulation instability," Nat. Communication **7**, 13675 (2016).

16. D. R. Solli, G. Herink, B. Jalali and C. Ropers, "Fluctuations and correlations in modulation Instability," Nature Photonics **6**, 463 (2012).

17. X. Wang, D. Bigourd, A. Kudlinski,K. K. Y. Wong, M. Douay, L. Bigot, A. Lerouge, Y. Quiquempois, and A. Mussot, "Correlation between multiple modulation instability side lobes in dispersion oscillating fiber," Opt. Lett. **39**, 1881 (2014).

18. T. Godin, B. Wetzel, T. Sylvestre, L. Larger, A. Kudlinski, A. Mussot, A. Ben Salem, M. Zghal, G. Genty, F. Dias, and J. M. Dudley, "Real time noise and wavelength correlations in octave-spanning supercontinuum generation," Opt. Exp. **21**, 18452 (2013).